Quantum phase transitions and Bose–Einstein condensation of magnons in hexagonal spin systems

2007 J. Phys.: Condens. Matter 19 386227

(http://iopscience.iop.org/0953-8984/19/38/386227)

IOP PUBLISHING JOURNAL OF PHYSICS: CONDENSED MATTER

J. Phys.: Condens. Matter **19** (2007) 386227 (11pp) doi:10.1088/0953-8984/19/38/386227

Quantum phase transitions and Bose–Einstein condensation of magnons in hexagonal spin systems

Han-Ting Wang and Yupeng Wang

Beijing National Laboratory of Condensed Matter Physics and Institute of Physics, Chinese Academy of Sciences, Beijing 100080, People's Republic of China

Received 30 April 2007, in final form 8 August 2007
Published 4 September 2007
Online at stacks.iop.org/JPhysCM/19/386227

Abstract

We study the $S = 1$ Heisenberg antiferromagnet with single-ion anisotropy in the hexagonal lattice using the bond-operator theory. The quantum phase transition from the spin singlet state to the ordered one and the field-induced long-range order in the perpendicular plane are shown to be described by the condensation of magnons. The results are compared with those from experiments using $AFeX_3$ (A = Cs, Rb and X = Cl, Br). The critical exponent α near H_{c1} is found to be about 1.144 in $CsFeCl_3$ and 1.599 in $CsFeBr_3$, which provides another route to study the dimensional crossover behavior in low-dimensional spin systems.

1. Introduction

Quantum spin systems have received considerable attention from both theoretical and experimental points of view. Recently, the quantum phase transition and the condensation of magnons have been extensively studied. Field-induced long-range order (LRO) in the plane perpendicular to the external magnetic field has been observed in many materials, such as $S = 1$ antiferromagnetic chains [1], antiferromagnetic spin dimers [2], even-leg spin ladders [3] and $S = \frac{1}{2}$ alternating chains [4], $S = 1$ three-dimensional antiferromagnets with large single-ion anisotropy $NiCl_2{\cdot}4SC(NH_2)_2$ [5] and coupled bilayer antiferromagnets $BaCuSi_2O_6$ [6, 7]. Theoretically, these experiments are interpreted with the idea of Bose–Einstein condensation of magnons [8, 9] and are analysed in detail with the methods of Bose–Einstein Hartree–Fock theory [10, 11], bond-operator mean-field theory [12, 13] and Monte Carlo simulations [14, 15].

On the other hand, the spin frustration effect often plays an important role in the magnetic ordering process. The frustrated spin system often shows infinite degeneracy in their classical ground state and quantum fluctuations are crucial to determine the ground states. For example, motivated by the recent experiments on Cs_2CuCl_4, the effect of the magnetic field is found to enhance the quantum fluctuation and to reduce the sublattice magnetization at the intermediate field in the anisotropic triangular antiferromagnet [16], and the incommensurability of the spin spiral phase increases with the external field [17]. The ground-state spin structures of $CsCuCl_3$ in a strong magnetic field were studied by mapping the problem onto the equivalent Bose gas problem [18]. In the following, we study the effects of the frustration on quantum phase

transitions and on Bose–Einstein condensation of magnons in the stacked triangular systems and compare the results with ABX_3-type hexagonal magnets.

At room temperature, members of the $AFeX_3$ family (with A = Rb and Cs, X = Cl, Br) have the same hexagonal structure with space group $P6_3/mmc$ and at low temperature they exhibit quasi-one-dimensional (1D) magnetic behavior. The magnetic interaction along the chains is stronger than that between the chains. In all cases the Fe^{2+} has an effective spin $S = 1$ and locally a singlet ground state with $m = 0$ due to the single ion anisotropy. If the exchange interaction is small compared to this anisotropy, the whole system has a singlet ground state (SGS) at $T \to 0$, which is the case for $CsFeCl_3$ and $CsFeBr_3$. While in $RbFeCl_3$ and $RbFeBr_3$, the total exchange energy is large enough to produce magnetic long-range order at low temperatures. In all Cl compounds the 1D exchange interaction is positive and creates ferromagnetic behavior along the chains; in contrast, in the Br compounds, this interaction is negative and thus antiferromagnetic behavior arises. The experimental studies on these materials were well reviewed by Collins and Petrenko [19].

Very recently, the field-induced magnetic order in the singlet ground state magnets $CsFeBr_3$ and $CsFeCl_3$ was experimentally investigated [20, 21] by magnetic neutron scattering and measurements of the magnetization and was discussed in the context of Bose–Einstein condensation of magnons. Concerning these experimental results, we study the $S = 1$ Heisenberg model with a single-ion anisotropy in the hexagonal lattice [19]:

$$H = \frac{1}{4}\sum_{\vec{r},\vec{\delta}_1}[J_0^{\perp}(S_{\vec{r}}^{+}S_{\vec{r}+\vec{\delta}_1}^{-} + S_{\vec{r}}^{-}S_{\vec{r}+\vec{\delta}_1}^{+}) + 2J_0^{\parallel}S_{\vec{r}}^{z}S_{\vec{r}+\vec{\delta}_1}^{z}] + \frac{1}{4}\sum_{\vec{r},\vec{\delta}_2}[J_1^{\perp}(S_{\vec{r}}^{+}S_{\vec{r}+\vec{\delta}_2}^{-} + S_{\vec{r}}^{-}S_{\vec{r}+\vec{\delta}_2}^{+}) + 2J_1^{\parallel}S_{\vec{r}}^{z}S_{\vec{r}+\vec{\delta}_2}^{z}] + D\sum_{\vec{r}}(S_{\vec{r}}^{z})^2 - g\mu_B B\sum_{\vec{r}}S_{\vec{r}}^{z}, \quad (1)$$

where $\sum_{\vec{r},\vec{\delta}_1}$ sums over the nearest neighbors along the chain and $\sum_{\vec{r},\vec{\delta}_2}$ in the triangular plane. An external magnetic field is applied with μ_B the Bohr magneton.

When $J_1^{\parallel} = J_1^{\perp} = 0$ and $J_0 > 0$, the model reduces to the $S = 1$ spin chain with large single-ion anisotropy and is extensively studied in connection with Haldane's fascinating conjecture [22]. During $D_{c1}(\sim -0.29) < D < D_{c2}(\sim 0.93)$, the system is in the Haldane phase. When $D > D_{c3}(\sim 1.01)$, the system is in the large-D phase [23, 24] with a singlet ground state and an excitation gap. While $J_0^{\parallel} = J_0^{\perp} = 0$, the model (1) describes an $S = 1$ antiferromagnet with large single-ion anisotropy in the triangular plane. The isotropic triangular antiferromagnet with $D = 0$ has a ground state of the 120° three sublattice structure [25]. Since in the limit of infinite D, the model (1) will be in the singlet state with all the spins in the state of $m = 0$, there exists a critical D_c denoting the transition from the large-D phase to the Néel phase in two and quasi-two dimensions. In the following, we use the bond operator formalism to study this quantum phase transition and the field-induced LRO of this model in the hexagonal lattice. In section 2 we give the self-consistent equations on the $S = 1$ Heisenberg model with single-ion anisotropy and then in sections 3 and 4, we study the quantum phase transitions induced by changing the physical parameters and by applying an external magnetic field, respectively. The experimental results are interpreted at the same time. A summary is given in section 5.

2. Self-consistent equations on the $S = 1$ Heisenberg model with single-ion anisotropy

For a single $S = 1$ spin, the spin operator can be represented as [26, 27] $S^{+} = \sqrt{2}(t_z^{\dagger}d + u^{\dagger}t_z)$, $S^{-} = \sqrt{2}(d^{\dagger}t_z + t_z^{\dagger}u)$ and $S^{z} = u^{\dagger}u - d^{\dagger}d$, where the three boson operators correspond to the three eigenstates $|\pm 1\rangle$ and $|0\rangle$: $|1\rangle = u^{\dagger}|\text{vac}\rangle$, $|0\rangle = t_z^{\dagger}|\text{vac}\rangle$, $|-1\rangle = d^{\dagger}|\text{vac}\rangle$ and $u^{\dagger}u + d^{\dagger}d + t_z^{\dagger}t_z = 1$.

Substituting the above boson representation into the original Hamiltonian (1) and assuming the t_z bosons are condensed, $\langle t_z\rangle = \langle t_z^\dagger\rangle = t$, we get

$$H = H(\text{chain}) + H(\text{plane}) + H(D) + H(h) + H(\mu) \tag{2}$$

with

$$\begin{aligned}
H(\text{chain}) &= \tfrac{1}{2}\sum_{\vec{r},\vec{\delta}_1}[J_0^\perp t^2(d_{\vec{r}}^\dagger d_{\vec{r}+\vec{\delta}_1} + u_{\vec{r}+\vec{\delta}_1}^\dagger u_{\vec{r}} + u_{\vec{r}} d_{\vec{r}+\vec{\delta}_1} + d_{\vec{r}}^\dagger u_{\vec{r}+\vec{\delta}_1}^\dagger + \text{h.c.}) \\
&\quad + J_0^\parallel (u_{\vec{r}}^\dagger u_{\vec{r}} - d_{\vec{r}}^\dagger d_{\vec{r}})(u_{\vec{r}+\vec{\delta}_1}^\dagger u_{\vec{r}+\vec{\delta}_1} - d_{\vec{r}+\vec{\delta}_1}^\dagger d_{\vec{r}+\vec{\delta}_1})] \\
H(\text{plane}) &= \tfrac{1}{2}\sum_{\vec{r},\vec{\delta}_2}[J_1^\perp t^2(d_{\vec{r}}^\dagger d_{\vec{r}+\vec{\delta}_2} + u_{\vec{r}+\vec{\delta}_2}^\dagger u_{\vec{r}} + u_{\vec{r}} d_{\vec{r}+\vec{\delta}_2} + d_{\vec{r}}^\dagger u_{\vec{r}+\vec{\delta}_2}^\dagger + \text{h.c.}) \\
&\quad + J_1^\parallel (u_{\vec{r}}^\dagger u_{\vec{r}} - d_{\vec{r}}^\dagger d_{\vec{r}})(u_{\vec{r}+\vec{\delta}_2}^\dagger u_{\vec{r}+\vec{\delta}_2} - d_{\vec{r}+\vec{\delta}_2}^\dagger d_{\vec{r}+\vec{\delta}_2})]
\end{aligned} \tag{3}$$

$$H(D) = D\sum_{\vec{r}}(u_{\vec{r}}^\dagger u_{\vec{r}} + d_{\vec{r}}^\dagger d_{\vec{r}})$$

$$H(h) = -h\sum_{\vec{r}}(u_{\vec{r}}^\dagger u_{\vec{r}} - d_{\vec{r}}^\dagger d_{\vec{r}})$$

$$H(\mu) = -\sum_{\vec{r}}\mu_{\vec{r}}(u_{\vec{r}}^\dagger u_{\vec{r}} + d_{\vec{r}}^\dagger d_{\vec{r}} + t^2 - 1)$$

where $h = g\mu_B B$ and a temperature-dependent chemical potential $\mu_{\vec{r}}$ is introduced to impose the constraint condition of single occupancy. By a mean-field approximation, we replace the local constraint by a global one and let $\mu_{\vec{r}} = \mu$. When t^2 is close to 1 or the density of the excitations is small, this approximation proves to be quite effective. It is pointed out that μ is still temperature-dependent. Making mean-field decoupling to the four operator terms

$$\begin{aligned}
(u_{\vec{r}}^\dagger u_{\vec{r}} - d_{\vec{r}}^\dagger d_{\vec{r}})(u_{\vec{r}+\vec{\delta}}^\dagger u_{\vec{r}+\vec{\delta}} - d_{\vec{r}+\vec{\delta}}^\dagger d_{\vec{r}+\vec{\delta}}) &= \tfrac{1}{2}(1 - t^2 + m)(u_{\vec{r}}^\dagger u_{\vec{r}} + u_{\vec{r}+\vec{\delta}}^\dagger u_{\vec{r}+\vec{\delta}}) \\
&\quad + \tfrac{1}{2}(1 - t^2 - m)(d_{\vec{r}}^\dagger d_{\vec{r}} + d_{\vec{r}+\vec{\delta}}^\dagger d_{\vec{r}+\vec{\delta}}) \\
&\quad - p(u_{\vec{r}} d_{\vec{r}+\vec{\delta}} + d_{\vec{r}} u_{\vec{r}+\vec{\delta}} + \text{h.c.}) - \tfrac{1}{2}(1 - t^2)^2 - \tfrac{1}{2}m^2 + 2p^2
\end{aligned} \tag{4}$$

with $m = \langle u_{\vec{r}}^\dagger u_{\vec{r}} - d_{\vec{r}}^\dagger d_{\vec{r}}\rangle$, $p_1 = \langle u_{\vec{r}} d_{\vec{r}+\vec{\delta}_1}\rangle$ and $p_2 = \langle u_{\vec{r}} d_{\vec{r}+\vec{\delta}_2}\rangle$ and after a Fourier–Bogoliubov transformation, we get the diagonalized Hamiltonian

$$H = \sum_k(\omega_k^{(1)}\alpha_k^\dagger\alpha_k + \omega_k^{(2)}\beta_k^\dagger\beta_k) + \sum_k\left(\omega_k - \frac{A_k + B_k}{2}\right) + E, \tag{5}$$

with

$$\begin{aligned}
\omega_k^{(1,2)} &= \omega_k \mp h \pm \tfrac{1}{2}(Z_1 J_0^\parallel + Z_2 J_1^\parallel)m \\
\omega_k &= \sqrt{\left(\frac{A_k + B_k}{2}\right)^2 - {C_k}^2} \\
A_k &= -\mu + D - h + \tfrac{1}{2}(Z_1 J_0^\parallel + Z_2 J_1^\parallel)(1 - t^2 + m) + Z_1 t^2 J_0^\perp \gamma_{1k} + Z_2 t^2 J_1^\perp \gamma_{2k} \\
B_k &= -\mu + D + h + \tfrac{1}{2}(Z_1 J_0^\parallel + Z_2 J_1^\parallel)(1 - t^2 - m) + Z_1 t^2 J_0^\perp \gamma_{1k} + Z_2 t^2 J_1^\perp \gamma_{2k} \\
C_k &= Z_1(t^2 J_0^\perp - J_0^\parallel p_1)\gamma_{1k} + Z_2(t^2 J_1^\perp - J_1^\parallel p_2)\gamma_{2k} \\
E &= \mu N(1 - t^2) - \tfrac{1}{4}NZ_1 J_0^\parallel[(1 - t^2)^2 + m^2 - 4p_1^2] - \tfrac{1}{4}NZ_2 J_1^\parallel[(1 - t^2)^2 + m^2 - 4p_2^2], \\
\gamma_{1k} &= \frac{1}{Z_1}\sum_{\delta_1} e^{i\vec{k}\cdot\vec{\delta}_1} \\
\gamma_{2k} &= \frac{1}{Z_2}\sum_{\delta_2} e^{i\vec{k}\cdot\vec{\delta}_2}
\end{aligned} \tag{6}$$

where $Z_1 = 2$ and $Z_2 = 6$ are the numbers of the nearest neighbors along the chain and in the plane, respectively. $\gamma_{1k} = \cos k_z$ and $\gamma_{2k} = \frac{1}{3}(\cos k_x + 2\cos\frac{1}{2}k_x \cos\frac{\sqrt{3}}{2}k_y)$ for the layered

triangular lattice. $\alpha_k = \chi_k u_k + \rho_k d^{\dagger}_{-k}$, $\beta_k = \chi_k d_{-k} + \rho_k u^{\dagger}_k$ with $\chi_k^2 = \frac{1}{2}(1 + \frac{A_k+B_k}{2\omega_k})$ and $\rho_k^2 = \frac{1}{2}(-1 + \frac{A_k+B_k}{2\omega_k})$. By analysing the excitation spectrum ω_k, we find that the energy gap occurs at $\vec{k}_0 = (\frac{4}{3}\pi, 0, \pi)$ for the antiferromagnetic intrachain interaction and at $\vec{k}_0 = (\frac{4}{3}\pi, 0, 0)$ for the ferromagnetic intrachain interaction, which corresponds to $CsFeBr_3$ and $CsFeCl_3$ respectively. The energy gap $\Delta = \omega_{\vec{k}_0}$. The ground state energy per site is $e_0 = \frac{1}{N}\sum_k(\omega_k - \frac{A_k+B_k}{2}) + \frac{1}{N}E$. The Gibbs free energy $G = Ne_0 - \frac{1}{\beta}\sum_k \ln[1 + n(\omega_k^{(1)})] - \frac{1}{\beta}\sum_k \ln[1 + n(\omega_k^{(2)})]$ with $n(\omega_k) = \frac{1}{e^{\beta\omega_k}-1}$ and $\beta = \frac{1}{k_B T}$. p_1, p_2, t^2, μ and m can be obtained by the saddle-point equations:

$$
\begin{aligned}
p_1 &= -\frac{1}{2N}\sum_k \frac{C_k}{\omega_k}\gamma_{1k}[1 + n(\omega_k^{(1)}) + n(\omega_k^{(2)})],\\
p_2 &= -\frac{1}{2N}\sum_k \frac{C_k}{\omega_k}\gamma_{2k}[1 + n(\omega_k^{(1)}) + n(\omega_k^{(2)})],\\
2 - t^2 &= \frac{1}{N}\sum_k \frac{A_k + B_k}{2\omega_k}[1 + n(\omega_k^{(1)}) + n(\omega_k^{(2)})],\\
\mu &= \frac{1}{N}\sum_k \frac{A_k + B_k - 2C_k}{2\omega_k}(Z_1 J_0^{\perp}\gamma_{1k} + Z_2 J_1^{\perp}\gamma_{2k})[1 + n(\omega_k^{(1)}) + n(\omega_k^{(2)})],\\
m &= \frac{1}{N}\sum_k [n(\omega_k^{(1)}) - n(\omega_k^{(2)})].
\end{aligned}
\tag{7}
$$

3. Quantum phase transition from the large-D state to the ordered state

For simplicity, we assume $J_0^{\parallel} = J_0^{\perp} = J_0$ and $J_1^{\parallel} = J_1^{\perp} = J_1$. At infinite D, all the spins will be in the state of $m = 0$ and there is an excitation gap from the singlet to the doublets. With decreasing D, the energy gap decreases and goes to zero at a critical D_c. With $t^2 = 1$, $\mu = 0$, $p_1 = 0$ and $p_2 = 0$, ω_k reduces to that from the spin wave theory and gives a rough estimation of $D_c = 4|J_0| + 6|J_1|$. We study the antiferromagnetic case $J_0 > 0$ first. In figure 1 (right axis), we show the changes of the energy gap with D for various $J_1 = 0.8J_0$, $J_1 = 0.5J_0$, $J_1 = 0.3J_0$, $J_1 = 0.1J_0$ and $J_1 = 0.015J_0$. The critical D_c decreases with decreasing J_1. However, there exists a critical $J_{1c} \sim 0.012J_0$, below which the energy gap keeps finite even at $D = 0$. In figure 2, we calculate the change of the energy gap for $J_1 = 0$ and $J_1 = 0.01J_0$. Δ/D changes little at large D and increases sharply at small D, which agrees well with the results obtained by Papanicolaou and Spathis with a modified semiclassical theory based on a $1/n$ expansion [28]. At large D, the energy gap mainly comes from the change from the singlet state of $m = 0$ to the doublets $m = \pm 1$ and is proportional to D; at small D, the energy gap (the Haldane gap) is mainly from the antiferromagnetic interaction. Therefore, the change of Δ/D gives us some indication of the transition from the large-D phase to the Haldane phase.

When $D < D_c$, the system enters into the ordered state. We assume part of the excitations are condensed at $\vec{k}_0$ [29]. Keeping $\omega_{\vec{k}_0} = 0$, we solve the self-consistent equations (7) with a BEC amount $n_0(T)$ extracted:

$$
\begin{aligned}
p_1 &= -\frac{C_{\vec{k}_0}}{A_{\vec{k}_0} + B_{\vec{k}_0}}\gamma_{1k_0} n_0(T) - \frac{1}{2N}\sum_k \frac{C_k}{\omega_k}\gamma_{1k}[1 + n(\omega_k^{(1)}) + n(\omega_k^{(2)})],\\
p_2 &= -\frac{C_{\vec{k}_0}}{A_{\vec{k}_0} + B_{\vec{k}_0}}\gamma_{2k_0} n_0(T) - \frac{1}{2N}\sum_k \frac{C_k}{\omega_k}\gamma_{2k}[1 + n(\omega_k^{(1)}) + n(\omega_k^{(2)})],\\
2 - t^2 &= n_0(T) + \frac{1}{N}\sum_k \frac{A_k + B_k}{2\omega_k}[1 + n(\omega_k^{(1)}) + n(\omega_k^{(2)})],
\end{aligned}
$$

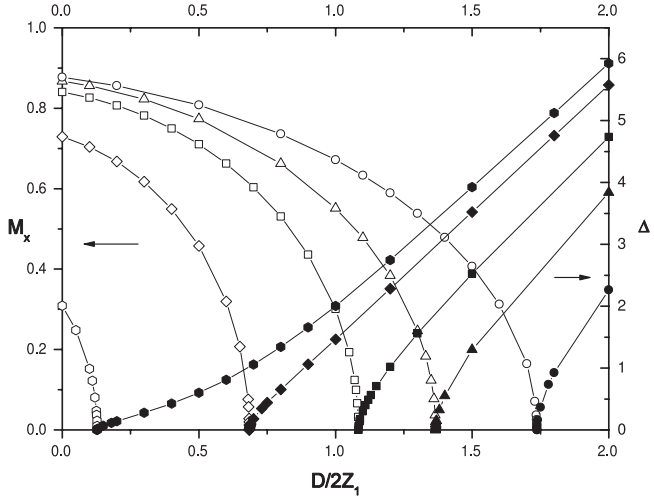

Figure 1. Changes of the energy gap (right axis) and the magnetization (left axis) with D for $J_1 = 0.8$ (circles), $J_1 = 0.5$ (triangles), $J_1 = 0.3$ (squares), $J_1 = 0.1$ (diamonds) and $J_1 = 0.015$ (hexagons), respectively. D and J_1 are in units of $J_0 > 0$.

$$\mu = \left(1 - \frac{2C_{\vec{k}_0}}{A_{\vec{k}_0} + B_{\vec{k}_0}}\right)(Z_1 J_0^{\perp}\gamma_{1\vec{k}_0} + Z_2 J_1^{\perp}\gamma_{2\vec{k}_0})n_0(T) + \frac{1}{N}\sum_k \frac{A_k + B_k - 2C_k}{2\omega_k}(Z_1 J_0^{\perp}\gamma_{1k} + Z_2 J_1^{\perp}\gamma_{2k})[1 + n(\omega_k^{(1)}) + n(\omega_k^{(2)})],$$
$$m = \frac{2\omega_{\vec{k}_0}}{A_{\vec{k}_0} + B_{\vec{k}_0}} n_0(T) + \frac{1}{N}\sum_k [n(\omega_k^{(1)}) - n(\omega_k^{(2)})]. \tag{8}$$

The magnetization induced by the condensation of magnons can be obtained by calculating $\langle S_{\vec{r}}^x\rangle$ and $\langle S_{\vec{r}}^y\rangle$ directly. We have $\langle S_{\vec{r}}^x\rangle = 2\sqrt{2}t\sqrt{n_0}\cos(\vec{k}_0\cdot\vec{r})$, $\langle S_{\vec{r}}^y\rangle = -2\sqrt{2}t\sqrt{n_0}\sin(\vec{k}_0\cdot\vec{r})$ and $\langle M_x\rangle = \sqrt{\langle S_{\vec{r}}^x\rangle^2 + \langle S_{\vec{r}}^y\rangle^2} = 2\sqrt{2}t\sqrt{n_0}$. Considering $\vec{k}_0 = (\frac{4}{3}\pi, 0, \pi)$ for the antiferromagnetic intrachain interaction and $\vec{k}_0 = (\frac{4}{3}\pi, 0, 0)$ for the ferromagnetic intrachain interaction, we get the 120° three sublattice spin structure. In figure 1 (left axis), we present the changes of $\langle M_x\rangle$ with D for $J_1 = 0.8J_0$, $J_1 = 0.5J_0$, $J_1 = 0.3J_0$, $J_1 = 0.1J_0$ and $J_1 = 0.015J_0$.

As mentioned above, when $J_1 < J_{1c}(\sim 0.012J_0)$, the energy gap keeps finite till $D = 0$, hence no quantum phase transition to the ordered state occurs. The existence of the critical J_{1c} indicates that only a finite interchain interaction can induce long-range order in the coupled $S = 1$ antiferromagnetic spin chains. This result is consistent with the studies on the two-dimensional array of weakly coupled antiferromagnetic spin chains. With the Schwinger-boson technique and the Wigner–Jordan transformation, it was shown that a finite coupling is necessary to introduce long-range antiferromagnetic order for the integer-spin case and an infinitesimal transverse coupling is enough for the half-integer-spin case [30].

When $J_1 \geqslant J_0 \geqslant 0$, the model (1) describes coupled triangular planes. The transition from the gapped disordered state to the Néel state occurs at larger D than that in the quasi-one-dimensional case. At $J_0 = J_1$, we get $D_c = 7.866J_1$ and at $J_0 = 0$, we have $D_c = 2.095J_1$.

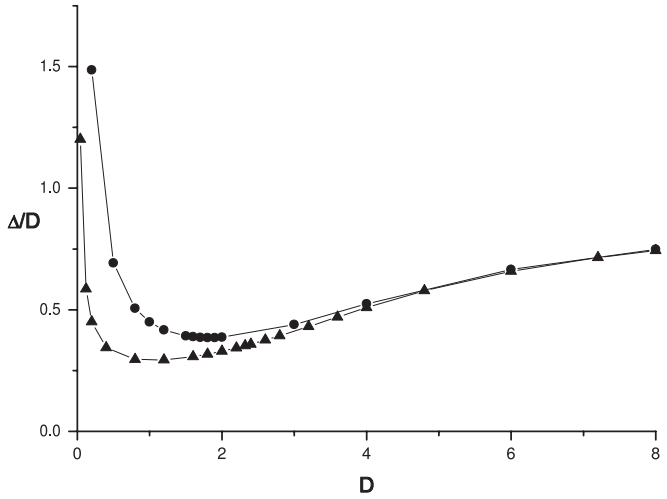

Figure 2. Changes of the energy gap Δ/D with D for $J_1 = 0$ (circles) and $J_1 = 0.01$ (triangles) respectively. D and J_1 are in units of $J_0 > 0$. The energy gap Δ/D changes little for large D and increases sharply for small D.

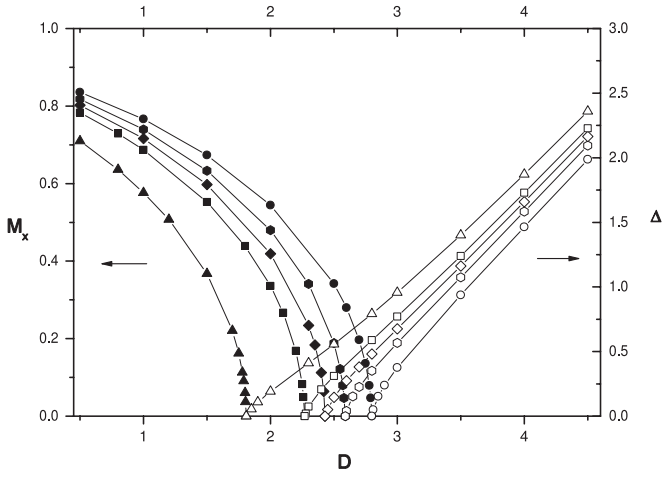

Figure 3. Changes of the energy gap Δ (right axis) and the magnetization M_x (left axis) with D for $J_1 = -0.03J_0$ (triangles), $-0.055J_0$ (squares), $-0.067J_0$ (diamonds), $-0.08J_0$ (hexagons) and $-0.1J_0$ (circles), respectively. $J_0 = -1$.

In the case of ferromagnetic intrachain interaction $J_0 < 0$ and antiferromagnetic interchain interaction $J_1 > 0$, the results are quite similar: a transition from the gapped large-D state to the ordered 120° state exists. In figure 3, we show the changes of the energy gap and the magnetization M_x with D for $J_1 = -0.03J_0$, $-0.055J_0$, $-0.067J_0$, $-0.08J_0$ and $-0.1J_0$ respectively. It should be pointed out that there should appear a ferromagnetic state at $D = 0$ and suitable J_1. Unfortunately, we cannot obtain this state since we start from the assumption of the condensation of t_z bosons (in the ferromagnetic state, most spins will be in the state of $m = 1$).

4. Long-range order induced by the external magnetic field

When an external magnetic field is applied in the chain direction, the excitations split and the component α_k decreases with increasing magnetic field as shown in equations (6). At a critical magnetic field $h_{c1} = \Delta_0$, the energy gap goes to zero. When the magnetic field further increases, part of the excitations condense. Consequently, a magnetization parallel to the external magnetic field appears and at the same time antiferromagnetic long-range order in the plane perpendicular to the magnetic field occurs. Similarly, we solve the self-consistent equations (7) with a BEC amount $n_h(T)$ extracted and $\omega_{1k_0} = 0$. The arrangement of the spins is still determined by $\vec{k}_0$. The magnetization in the perpendicular plane is $\langle M_x \rangle = \sqrt{2}t\sqrt{n_h}\sqrt{1 - \frac{2C_{k_0}}{A_{k_0}+B_{k_0}}}$, where n_h is the condensed density induced by the magnetic field. At a second critical magnetic field h_{c2}, the parallel magnetization saturates and the antiferromagnetic LRO in the perpendicular plane disappears. With $p_1 = p_2 = 0$, $m = 1$ and $t = 0$, an estimation of h_{c2} gives $h_{c2} = D + Z_1(J_0^{\parallel} + |J_0^{\perp}|) + Z_2(J_1^{\parallel} + \frac{1}{2}J_1^{\perp})$. For a given magnetic field $h_{c2} > h > h_{c1}$, we can get a critical temperature $T_c(h)$, at which the energy gap and the condensed density $n_h(T)$ are both zero.

We study $CsFeCl_3$ and $RbFeCl_3$ first. $CsFeCl_3$ and $RbFeCl_3$ have ferromagnetic interaction along the c-axis and antiferromagnetic interaction in the triangular plane. Depending on the relative magnitudes of the exchange interaction and the large D term, $CsFeCl_3$ and $RbFeCl_3$ show remarkably different magnetic properties at low temperatures. $CsFeCl_3$ has a nonmagnetic ground state at zero magnetic field. When an external magnetic field is applied along the c-axis, field-induced three-dimensional long-range order appears in the field region of 4 T $\leqslant H \leqslant$ 11 T at $T_N \leqslant 2.6$ K [31]. While $RbFeCl_3$ reveals three-dimensional long-range order below $T_N = 2.55$ K [32]. Very recently, the field-induced magnetic order in $CsFeCl_3$ was studied by the measurements of the magnetization $M_{\parallel}$ and the magnetic neutron scattering from $M_{\perp}$ [21]. In particular, the field dependence of $M_{\perp}$ was clearly shown to be described by the order parameter $\langle S_x \rangle$ and the incommensurate–commensurate phase transition was observed in the field region of 5 T $< H <$ 6 T. The phase diagrams of $CsFeCl_3$ in the H–T plane were extensively studied experimentally [21, 31, 33] and theoretically by the dynamical correlated-effective-field theory (DCEFT) [36]. Since the physical parameters from different groups are quite different, we solve equations (7) with several sets of parameters and try to study the effects of every physical parameter. In figure 4, we show the phase diagrams in the H–T plane with $J_0 = -1$, $J_1 = 0.055$, 0.067, 0.08 and $D = 3$, 4, 5, respectively. The critical temperature T_c increases quickly with increasing J_1 and the critical magnetic fields h_{c1} and h_{c2} are mainly decided by D. Relatively, the parameters of $J_1 = 0.067|J_0|$ and $D = 4|J_0|$ with $J_0 = -4.11$ K can give good results compared with the experimental data. For example, the critical magnetic field $H_{c1} = 1.659|J_0| = 4.0T$ and $H_{c2} = 4.603|J_0| = 11.1$ T with $g_{\parallel} = 2.54$. However, the values of T_c are lower than those of the experiments.

Near h_{c1}, we fit the results with $h_{c1}(T) - h_{c1}(0) \propto T^{\alpha}$ with $J_1 = 0.067|J_0|$ and $D = 4|J_0|$. We get $\alpha \approx 1.144$, which are much smaller than those of the unfrustrated three-dimensional systems [10, 11, 13–15]. We further calculate the changes of α with various interchain interactions J_1. Up to $J_1 = 0.25|J_0|$, α is nearly the same (for $|J_0/J_1| = 0.01$, 0.03, 0.067, 0.1, 0.2, and 0.25, we get $\alpha = 1.140$, 1.142, 1.144, 1.160, 1.177 and 1.209, respectively). The dimensional crossover behavior at a quantum critical point is currently an interesting topic in the subject of Bose–Einstein condensation of magnons [34, 35]. $CsFeCl_3$, with ferromagnetic interaction along the chain, provides us with another real material to use when studying this problem.

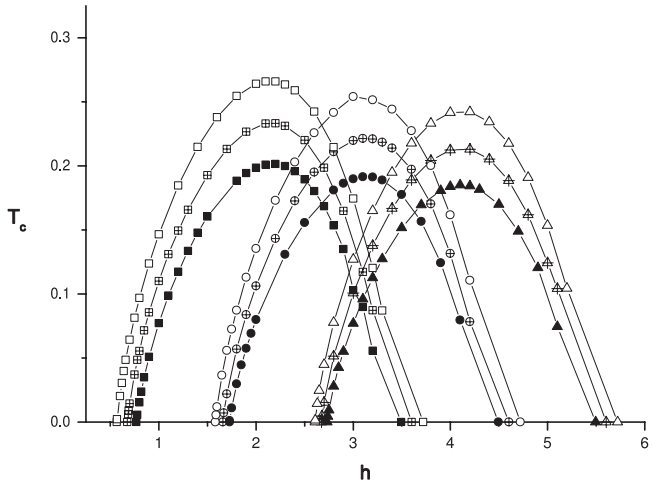

Figure 4. Critical temperature $T_c(h)$ for $CsFeCl_3$ with $J_1 = -0.055J_0$ (black symbols), $-0.067J_0$ (symbols with crosses), $-0.08J_0$ (white symbols) and $D = 3$ (squares), $D = 4$ (circles) and $D = 5$ (triangles). The temperature and the magnetic field $h(= g\mu_B B)$ are in units of $|J_0| = 1$.

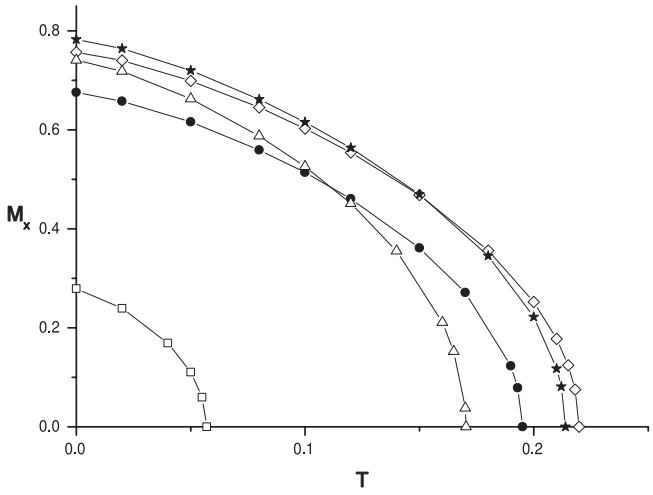

Figure 5. Changes of the field-induced magnetization M_x with temperatures at $h = 1.8$ (squares), 2.6 (triangles), 3. (diamonds), 3.4 (stars) and 3.8 (circles) in $CsFeCl_3$, where $J_1 = 0.067|J_0|$ and $D = 4|J_0|$. The temperature and the magnetic field $h(= g\mu_B B)$ are in units of $|J_0|$.

In figure 5, we show the changes of M_x with temperature and magnetic field for $J_1 = 0.067|J_0|$ and $D = 4|J_0|$.

$RbFeCl_3$ reveals three-dimensional LRO below $T_N = 2.55$ K. As a comparison, we give its phase diagram in figure 6 with $J_0^{\perp} = -1$, $J_0^{\parallel} = -1.3$, $J_1^{\perp} = -0.085J_0^{\perp}$, $J_1^{\parallel} = -0.085J_0^{\parallel}$ and $D = 2$. The parameters are from Suzuki's DCEFA theory [37].

Different from $CsFeCl_3$ and $RbFeCl_3$, $CsFeBr_3$ and $RbFeBr_3$ have antiferromagnetic interaction along the c-axis and antiferromagnetic interaction in the triangular plane. The ground state of $CsFeBr_3$ is a spin singlet due to the large single-ion anisotropy. The interaction parameters determined by different research groups are different. Considering most groups

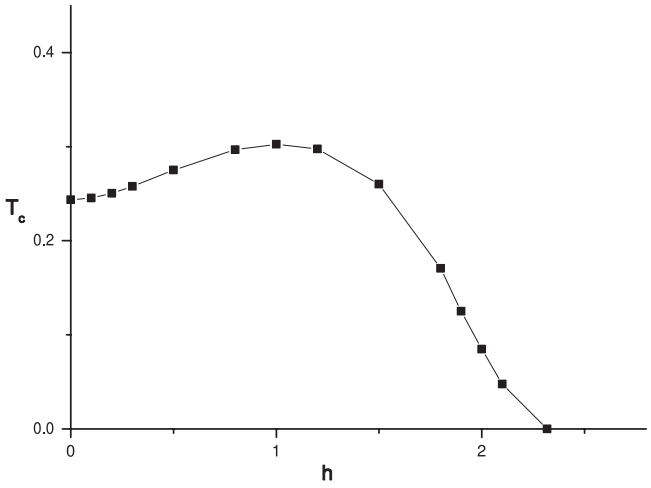

Figure 6. Critical temperature $T_c(h)$ for $RbFeCl_3$. The physical parameters are chosen as $J_0^{\perp} = -1$, $J_0^{\parallel} = -1.3$, $J_1^{\perp} = -0.085J_0^{\perp}$, $J_1^{\parallel} = -0.085J_0^{\parallel}$ and $D = 2$. The temperature and the magnetic field $h(= g\mu_B B)$ are in units of $|J_0^{\perp}|$.

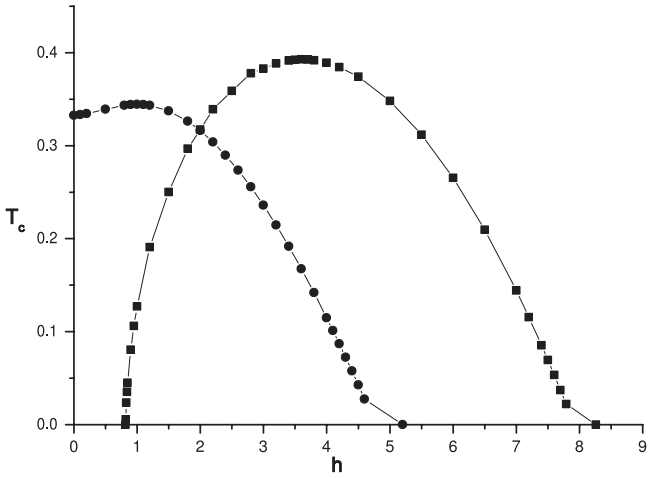

Figure 7. Critical temperature $T_c(h)$ for $CsFeBr_3$ (squares) and $RbFeBr_3$ (circles). For $CsFeBr_3$, $J_1 = 0.1J_0$ and $D = 3.36J_0$. The temperature and the magnetic field $h(= g\mu_B H)$ are in units of J_0 and $J_0 = 6.4$ K. For $RbFeBr_3$, the physical parameters are chosen as $J_0^{\perp} = 0.67J_0^{\parallel}$, $J_1^{\parallel} = 0.1J_0^{\parallel}$, $J_1^{\perp} = 0.1J_0^{\perp}$ and $D = 0.8625J_0^{\parallel}$. The temperature and the magnetic field $h(= g\mu_B B)$ are in units of $J_0^{\parallel}$.

gave $J_0^{\perp} \approx J_0^{\parallel}$ and $J_1^{\perp} \approx J_1^{\parallel}$ [19, 20, 38], we set $J_0^{\perp} = J_0^{\parallel}$ and $J_1^{\perp} = J_1^{\parallel}$ and extract the parameters as $J_0 = 6.4$ K, $J_1 = 0.1J_0$ and $D = 3.36J_0 = 21.5$ K. Solving equations (7), we have $\Delta = 0.818\,88J_0 = 5.24$ K and $H_{c2} = 8.26J_0 = 52.86$ K, which agrees well with the experimental data $H_{c1} = 2.89$ T $= 5.242$ K and $H_{c2} = 27.8$ T $= 54$ K with $g_{\parallel} = 2.7$. In figure 7 (curve with squares), we show the phase diagram in the H–T plane. This is in agreement with the experimental results obtained by magnetic susceptibility, the magnetization process and specific measurements [20] and by an NMR experiments [39]. Fitting the data with

$h_{c1}(T) - h_{c1}(0) \propto T^{\alpha}$ near h_{c1}, we find $\alpha \sim 1.599$, which is consistent with $\phi_2 = 1.8$ obtained near H_{N2} in $CsFeBr_3$ [20].

In $RbFeBr_3$, three-dimensional long-range order is realized at 5.5 K because of the strong intrachain exchange interaction compared with the crystalline field splitting together with weak interchain interaction [40]. As a comparison, in figure 7 (curve with circles), we show the critical temperature as a function of magnetic field, where the physical parameters are chosen as [40, 41] $J_0^{\perp} = 0.67 J_0^{\parallel}$, $J_1^{\parallel} = 0.1 J_0^{\parallel}$, $J_1^{\perp} = 0.1 J_0^{\perp}$ and $D = 0.8625 J_0^{\parallel}$. Although the phase diagrams of $CsFeCl_3$ and $RbFeCl_3$ were largely studied experimentally and theoretically and of $CsFeBr_3$ experimentally, the phase diagram of $RbFeBr_3$ is seldom studied.

The magnetic dipole–dipole interaction in $CsFeCl_3$ and $RbFeCl_3$ with ferromagnetic intrachain interaction may play an important role. The incommensurate–commensurate phase transition in the magnetic field [21, 32] was attributed to this interaction by Shiba [42] and to the spin fluctuations by Lindgård [43]. Both the transverse and the longitudinal spin fluctuations were argued to be responsible for the two-step phase transition observed in $CsFeBr_3$ [20]. The lattice deformation or structure phase transition was observed in $CsFeCl_3$ [21] and $RbFeBr_3$ [44]. To give an intuitive and unified theory within the context of Bose–Einstein condensation of magnons, we do not consider these subtle effects in our studies.

5. Summary

In summary, we have studied the $S = 1$ Heisenberg antiferromagnet with single-ion anisotropy in the layered triangular lattice by the bond-operator theory. The quantum phase transition from the spin singlet state to the ordered one and the field-induced long-range order in the perpendicular plane are shown to be described by the condensation of magnons. In comparison with the experimental results on $AFeX_3$ (A = Cs, Rb and X = Cl, Br), we calculate the phase diagram, the field-induced staggered magnetization and the critical exponent near H_{c1}. The exponent α are found to be about 1.144 in $CsFeCl_3$ and 1.599 in $CsFeBr_3$, which provides another route to study the dimensional crossover behavior in the low-dimensional spin systems.

Acknowledgments

We acknowledge the financial support from the Natural Science Foundation of China and 973-project under grant nos. 2006CB921300 and 2006CB921400.

References

[1] Ajiro Y, Goto T, Kikuchi H, Sakakibara T and Inami T 1989 *Phys. Rev. Lett.* **63** 1424
Honda Z, Katsumata K, Katori H A, Yamada K, Lhishi T, Manabe T and Yamashita M 1997 *J. Phys.: Condens. Matter* **9** L83
Honda Z, Asakawa H and Katsumata K 1998 *Phys. Rev. Lett.* **81** 2566

[2] Oosawa A, Ishii H and Tanaka H 1999 *J. Phys.: Condens. Matter* **11** 265
Oosawa A, Aruga Katori H and Tanaka H 2001 *Phys. Rev.* B **63** 134416
Oosawa A, Takamasu T, Tatani K, Abe H, Tsujii N, Suzuki O, Tanaka H, Kido G and Kindo K 2002 *Phys. Rev.* B **66** 104405
Cavadini N, Ruegg Ch, Furrer A, Gudel H U, Kramer K, Mutka H and Vorderwisch P 2002 *Phys. Rev.* B **65** 132415
Ruegg C, Cavadini N, Furrer A, Gudel H U, Kramer K, Mutka H, Wildes A, Habicht K and Vorderwisch P 2003 *Nature* **423** 62

[3] Chaboussant G, Fagot-Revurat Y, Julien M H, Hanson M E, Berthier C, Horvatic M, Levy L P and Piovesana O 1998 *Phys. Rev. Lett.* **80** 2713
Mayaffre H, Horvatic H, Berthier C, Julien M H, Segransan P, Levy L and Piovesana O 2000 *Phys. Rev. Lett.* **85** 4795
Mito M, Akama H, Kawae T, Takeda K, Deguchi H and Takagi S 2002 *Phys. Rev.* B **65** 104405

[4] Manaka H, Yamada I, Honda Z, Katori H A and Katsumata K 1998 *J. Phys. Soc. Japan* **67** 3913
Hammar P R, Reich D H, Broholm C and Trouw F 1998 *Phys. Rev.* B **57** 7846
Stone M B, Zaliznyak I, Reich D H and Broholm C 2001 *Phys. Rev.* B **64** 144405
Tennant D A, Broholm C, Reich D H, Nagler S E, Granroth G E, Barnes T, Damle K, Xu G, Chen Y and Sales B C 2003 *Phys. Rev.* B **67** 054414
[5] Paduan-Filho A, Gratens X and Oliveira N F Jr 2004 *Phys. Rev.* B **69** 020405(R)
Paduan-Filho A, Gratens X and Oliveira N F Jr 2004 *J. Appl. Phys.* **95** 7537
Zapt V S, Zocco D, Hansen B R, Jaime M, Harrison N, Batista C D, Kenzelmann M, Niedermayer C, Lacerda A and Paduan-Filho A 2006 *Phys. Rev. Lett.* **96** 077204
[6] Jaime M, Correa V F, Harrison N, Batista C D, Kawashima N, Kazuma Y, Jorge G A, Stein R, Heinmaa I, Zvyagin S A, Sasago Y and Uchinokura K 2005 *Phys. Rev. Lett.* **93** 087203
[7] Sebastian S E, Sharma P A, Jaime M, Harrison N, Correa V, Balicas L, Kawashima N, Batista C D and Fisher I R 2005 *Phys. Rev.* B **72** 100404
[8] Matsubara T and Matsuda H 1956 *Prog. Theor. Phys.* **16** 569
[9] Affleck I 1991 *Phys. Rev.* B **43** 3215
[10] Nikuni T, Oshikawa M, Oosawa A and Tanaka H 2000 *Phys. Rev. Lett.* **84** 5868
[11] Misguich G and Oshikawa M 2004 *J. Phys. Soc. Japan* **73** 3429
[12] Matsumoto M, Normand B, Rice T M and Sigrist M 2002 *Phys. Rev. Lett.* **89** 077203
[13] Wang H-T and Wang Y 2005 *Phys. Rev.* B **71** 104429
[14] Wessel S, Olshanii M and Haas S 2001 *Phys. Rev. Lett.* **87** 206407
Nohadani O, Wessel S, Normand B and Haas S 2004 *Phys. Rev.* B **69** 220402(R)
[15] Kawashima N 2004 *J. Phys. Soc. Japan* **73** 3219
[16] Gan J Y, Zhang F C and Su Z B 2003 *Phys. Rev.* B **67** 144427
[17] Shen S Q and Zhang F C 2002 *Phys. Rev.* B **66** 172407
[18] Nikuni T and Shiba H 2001 *J. Phys. Soc. Japan* **70** 3068
[19] Collins M F and Petrenko O A 1997 *Can. J. Phys.* **75** 605
[20] Tanaka Y, Tanaka H, Ono T, Oosawa A, Morishita K, Iio K, Kato T, H, Katori A, Bartashevich M I and Goto T 2001 *J. Phys. Soc. Japan* **70** 3068
[21] Toda M, Fuji Y, Kawano S, Goto T, Chiba M, Ueda S, Nakajima K, Kakurai K, Klenke J, Feyerheim R, Meschke M, Graf H A and Steiner M 2005 *Phys. Rev.* B **71** 224426
[22] Haldane F D M 1983 *Phys. Rev. Lett.* **50** 1153
[23] Botet R, Jullien R and Kolb M 1983 *Phys. Rev.* B **28** 3914
[24] Sakai T and Takahashi M 1990 *Phys. Rev.* B **42** 4537
[25] Jolicoeur Th and Le Guillou J C 1989 *Phys. Rev.* B **40** 2727
Singh R R P and Huse D A 1992 *Phys. Rev. Lett.* **68** 1766
[26] Sachdev S and Bhatt R N 1990 *Phys. Rev.* B **41** 9323
[27] Wang H-T, Shen J-L and Su Z-B 1997 *Phys. Rev.* B **56** 14435
[28] Papanicolaou N and Spathis P 1990 *J. Phys.: Condens. Matter* **2** 6575
[29] Hirsch J E and Tang S 1989 *Phys. Rev.* B **39** 2850
Sarker S, Jayaprakash C, Krishnamurthy H R and Ma M 1989 *Phys. Rev.* B **40** 5028
[30] Azzouz M and Douçot 1993 *Phys. Rev.* B **47** 8660
Azzouz M 1993 *Phys. Rev.* B **48** 6136
[31] Haseda T, Wada N, Hata M and Amaya K 1981 *Physica* B and C **108B** 841
[32] Wada N, Sumiyoshi K, Watanabe T and Amaya K 1983 *J. Phys. Soc. Japan* **52** 1893
Wada N, Ubukoshi K and Hirakawa K 1982 *J. Phys. Soc. Japan* **51** 2833
[33] Chiba M, Ueda S, Yanagimoto T, Toda M and Goto T 2000 *Physica* B **284–288** 1529
[34] Sebastian S E, Harrison N, Batista C D, Balicas L, Jaime M, Sharma P A, Kawashima N and Fisher I R 2006 *Nature* **441** 617
[35] Wang H-T, Xu B and Wang Y 2006 *J. Phys.: Condens. Matter* **18** 4719
[36] Suzuki N and Makino J 1995 *J. Phys. Soc. Japan* **64** 2166
[37] Suzuki N 1990 *J. Phys. Soc. Japan* **52** 2947
[38] Harrison A and Visser D 1992 *J. Phys.: Condens. Matter* **4** 6977
[39] Makamura T, Ishida T, Fujii Y, Kikuchi H, Chiba M, Kubo T, Yamamoto Y and Hori H 2003 *Physica* B **329–333** 864
[40] Adachi K, Takeda K, Matsubara F, Mekata M and Haseda T 1983 *J. Phys. Soc. Japan* **52** 2202
[41] Lines M E and Eibschütz M 1975 *Phys. Rev.* B **11** 4583
[42] Nikuni T and Jacobs A E 2000 *J. Phys. Soc. Japan* **69** 1484
[43] Lindgård P A and Schmid B 1993 *Phys. Rev.* B **48** 13636
[44] Mitsui T, Machida K, Kato T and Iio K 1994 *J. Phys. Soc. Japan* **63** 839